# Supplementary Methods and Materials

## Title: deepDR: A network-based deep learning approach to *in silico* drug repositioning

**Zeng et al., Bioinformatics 2019**

*To whom correspondence should be addressed:

Feixiong Cheng, PhD

Genomic Medicine Institute

Lerner Research Institute, Cleveland Clinic

9500 Euclid Avenue, Cleveland, Ohio 44195

Email: chengf@ccf.org

Phone: +1-216-4447654

Fax: +1-216-6361609

## Table of contents

Supplementary Information files contain Supplemental Methods, 9 Supplementary Tables, one Supplemental Figures, one Supplementary Database, and Supplementary References.

**Details for reconstruction of experimentally validated drug-target interaction network**

We collected high-quality physical drug-target interactions on FDA-approved drugs from 6 commonly used data sources, and defined a physical drug-target interaction using reported binding affinity data: inhibition constant/potency ($K_i$), dissociation constant ($K_d$), median effective concentration ($EC_{50}$), or median inhibitory concentration ($IC_{50}$) ≤ 10 μM. Drug-target interactions were acquired from the DrugBank database (v4.3) [1], the Therapeutic Target Database (TTD, v4.3.02) [2], and the PharmGKB database [3]. Specifically, bioactivity data of drug-target pairs were collected from three widely used databases: ChEMBL (v20) [4], BindingDB [5], and IUPHAR/BPS Guide to PHARMACOLOGY [6]. After extracting the bioactivity data related to drugs from these databases, we retained only the drug-target interactions that meet the following three criteria: (i) binding affinities, including $K_i$, $K_d$, $IC_{50}$ or $EC_{50}$ each ≤ 10 μM; (ii) human proteins can be represented by unique UniProt accession number; and (iii) proteins are marked as 'reviewed' in the UniProt database [7]. In total, 6,744 drug-target interactions connecting 1,519 FDA-approved drugs and 1,025 unique human targets (proteins) were used (**Table S1, S2**).

**Collection of the clinically reported drug-drug interactions**

We compiled clinically reported DDI data from the DrugBank database (v4.3) [1]. Chemical name, generic name or commercial name of each drug were

standardized by Medical Subject Headings (MeSH) and Unified Medical Language System (UMLS) vocabularies [8] and further transferred to DrugBank ID from the DrugBank database (v4.3) [1]. In total, 290,836 clinically reported DDIs connecting 1,519 unique drugs were retained.

**Description of re-constructing drug-side effect network**

We collected the clinically reported drug side effects or adverse drug event (ADE) information by assembling data from MetaADEDB [9], CTD [10], SIDER (version 2) [11], and OFFSIDES [12]. Only ADE data with clinically reported evidence were used. All drugs and ADE items in MetaADEDB were annotated using Medical Subject Headings (MeSH) and Unified Medical Language System (UMLS) vocabularies. And, duplicated drug−ADE associations were excluded. In total, 382,041 drug−ADE associations collecting 1,519 approved drugs and 12,904 ADEs were used in this study.

**Chemical similarity analysis of drug pairs**

We downloaded chemical structure information (SMILES format) from the DrugBank database and computed MACCS fingerprints of each drug using Open Babel v2.3.1 [13]. If two drug molecules have *a* and *b* bits set in their MACCS fragment bit-strings, with *c* of these bits being set in the fingerprints of both drugs, the Tanimoto coefficient (*T*) of a drug-drug pair is defined as:

$$T = \frac{c}{a+b-c} \quad \text{(S1)}$$

*T* is widely used in drug discovery and development [14], offering a value in the range of zero (no bits in common) to one (all bits are the same).

**Drug side effects' similarity measure**

For drug side effects' similarity, each drug is coded using side effect bit vectors. Each bit represents one type of side effect. If a side effect event is associated with a drug in the drug-side effect network, the corresponding bit will be set to '1', otherwise '0'. Then, the $S_{SE}(a,b)$ between drug $d_a$ and $d_b$ is calculated using the Tanimoto coefficient (Eq. S1) by inputting the drug's side effect bit vectors.

**Protein sequence similarity (identity) analysis**

***Data resource.*** We downloaded the canonical protein sequences of drug targets (proteins) in *Homo sapiens* from Uniprot database (http://www.uniprot.org/).

***Similarity of drug targets.*** We calculated the protein sequence similarity $S_p(a,b)$ of two drug targets *a* and *b* using the Smith-Waterman algorithm [15]. The Smith-Waterman algorithm performs local sequence alignment by comparing segments of all possible lengths and optimizing the similarity

measure for determining similar regions between two strings of protein canonical sequences of drug targets.

***Similarity of drug pairs.*** The overall sequence similarity of the drug targets binding two drugs *A* and *B* is determined by equation (S2) by averaging all pairs of proteins *a* and *b* with $a \in A$ and $b \in B$ under the condition $a \neq b$. This condition ensures that for drugs with common targets we do not take pairs into account where a target would be compared to itself.

$$< S_p >= \frac{1}{n_{pairs}} \sum_{\{a,b\}} S_p(a,b) \quad \text{(S2)}$$

**Gene Ontology (GO) similarity analysis for drug targets**

***Data source.*** The Gene Ontology (GO) annotation for all drug target-coding genes are downloaded from website: http://www.geneontology.org/. We used three types of the experimentally validated or literature-derived evidences: *biological processes (BP)*, *molecular function (MF)*, and *cellular component (CC)*, excluding annotations inferred computationally.

***Similarity of drug targets.*** The semantic comparison of GO annotations provides quantitative ways to compute similarities between genes and gene products. We computed GO similarity $S_{GO}(a,b)$ for each pair of drug target-coding genes *a* and *b* using a graph-based semantic similarity measure algorithm[16] implemented in an R package, named GOSemSim [17]. In this study, three types of pairwise drug targets' GO similarities were used: BP, MF, and CC.

***Similarity of drug pairs.*** The overall GO similarity of the drug target-coding genes binding to two drugs *A* and *B* is determined by equation (S3), averaging all pairs of drug target-coding genes *a* and *b* with $a \in A$ and $b \in B$.

$$< S_{GO} >= \frac{1}{n_{pairs}} \sum_{\{a,b\}} S_{GO}(a,b) \quad \text{(S3)}$$

Here three types of pairwise drugs' GO similarities were used: BP, MF, and CC.

**Clinical similarity analysis for drug pairs**

Clinical similarities of drug pairs derived from the drug Anatomical Therapeutic Chemical (ATC) classification systems codes have been commonly used to predict new drug targets [9]. The ATC codes for all FDA-approved drugs used in this study were downloaded from the DrugBank database (v4.3) [1]. The *k*th level drug clinical similarity ($S_k$) of drugs *A* and *B* is defined via the ATC codes as below.

$$S_k(A,B) = \frac{\mathrm{ATC}_k(A) \cap \mathrm{ATC}_k(B)}{\mathrm{ATC}_k(A) \cup \mathrm{ATC}_k(B)} \quad \text{(S4)}$$

where $\mathrm{ATC}_k$ represents all ATC codes at the *k*th level. A score $S_{atc}(A,B)$ is used to define the clinical similarity between drugs *A* and *B*:

$$S_{atc}(A,B) = \frac{\sum_{k=1}^{n} S_k(A,B)}{n} \quad \text{(S5)}$$

Where n represents the five levels of ATC codes (ranging from 1 to 5). Note that drugs can have multiple ATC codes. For example, nicotine (a potent parasympathomimetic stimulant) has four different ATC codes: N07BA01, A11HA01, C04AC01, C10AD02. For a drug with multiple ATC codes, the clinical

similarity was computed for each ATC code, and then, the average clinical similarity was used.

**Details when getting the PPMI matrix of each network**

For homogeneous networks (e.g., drug-drug interaction network) and six similarity networks, we get the PPMI matrix of each network by directly running the first step of deepDR model on each of these networks. For heterogeneous networks, i.e., drug-target, drug-side-effect, we construct the corresponding similarity networks based on the Jaccard similarity coefficient first, and then run the first step of deepDR model on these similarity networks. Jaccard similarity is a common statistic used for characterizing the similarity and diversity between two sets of samples. Taking the drug-side-effect association network as an example, we use the following formula to measure the similarity between drug $i$ and drug j:

$$Sim(i,j) = \frac{|SE_i \cap SE_j|}{|SE_i \cup SE_j|} \quad \text{(S6)}$$

Where $SE_i$ denotes the set of side-effects of drug $i$. Then we run the first step of deepDR model on this similarity network to obtain the PPMI matrix.

**Hyperparameter Selection**

In our experiments, we set ω=0.98, and T= 3 (the number of RW steps) in the RWR step of deepDR. In MDA step, the number of training epochs is 100, the batch size is 64. We chose binary cross entropy as loss function. We used

sigmoid function as the activation function and used the stochastic gradient descent with the default learning rate 0.01 to perform gradient descent. The architecture of MDA is [9*1519, 9*1000, 9*500, 9*100]. In cVAE, we chose the architecture [1519,1000,100], the learning rate is 0.001. Specifically, in the pretraining step of cVAE, we selected α from 1,2,…,10 and β from 0,0.1,0.2,…,1. We finally used α=6 and β=0.1. In the refinement step of cVAE, we selected α from 1,2,…,15 and β from 0,0.5,1,…,3. We finally used α=8 and β=0.5 . We tune α and β with larger values for the sparsity in refinement.

**Baseline Methods**

We compared the performance of deepDR with that of several start-of-the-art prediction methods, including DTINet [18], KBMF [19], RWR [20, 21], Katz [22], RF [23], SVM [24]. DTINet, KBMF are matrix factorization methods. RWR, Katz are network-based prediction methods, and RF, SVM are machine learning-based methods. Both RF and SVM need preprocessed features for classification, we use PCA (principal components analysis) to obtain low-dimensional informative features for drugs and diseases. Specifically, in order to get feature representations of different networks, we extract features from 9 drug-related networks and one disease-protein association network, each network we extract 100-dimensional feature vectors, and put them together. Later we use SVM and Random Forest for classification. While RWR and Katz are not particularly designed to exploit multiple drug network data for prediction.

To compare our method with these methods, we calculate a disease similarity network from the Jaccard similarity of disease-protein association network, and choose drug chemical similarity for them.

For the hyperparameters used in the baseline methods, we tuned them to get the best performance in the cross validation. In DTINet, we chose $f_{drug}$ from {100,150,…,300}, and $f_{disease}$ from {100,200,…,1000}. For KBMF, the subspace dimensionality parameter R was chosen from {5,10, …,40}. In RWR, the probability of restart ω was chosen from {0.0, 0.1, …,1.0}, the number of RW steps T was chosen from {2,3, …,25}. In Katz, the number of walks was chosen from {1,2,3,4}, and the non-negative coefficient β which dampens contributions from longer walks was chosen from {0.0, 0.01, …,0.1, …,1.0}. For Random forest, we chose the number of trees from {100,200, …,1000}. For SVM, the optimal hyperparameters of the SVM (the weight regularization parameter C and λ in the RBF kernal) were determined by a grid search, and were both chosen from $\{2^{-4}, 2^{-3}, \ldots, 2^{4}\}$. A soft margin SVM with radial basis function (RBF) kernel in the Gaussian form was used in our experiments.

# Supplementary Figures

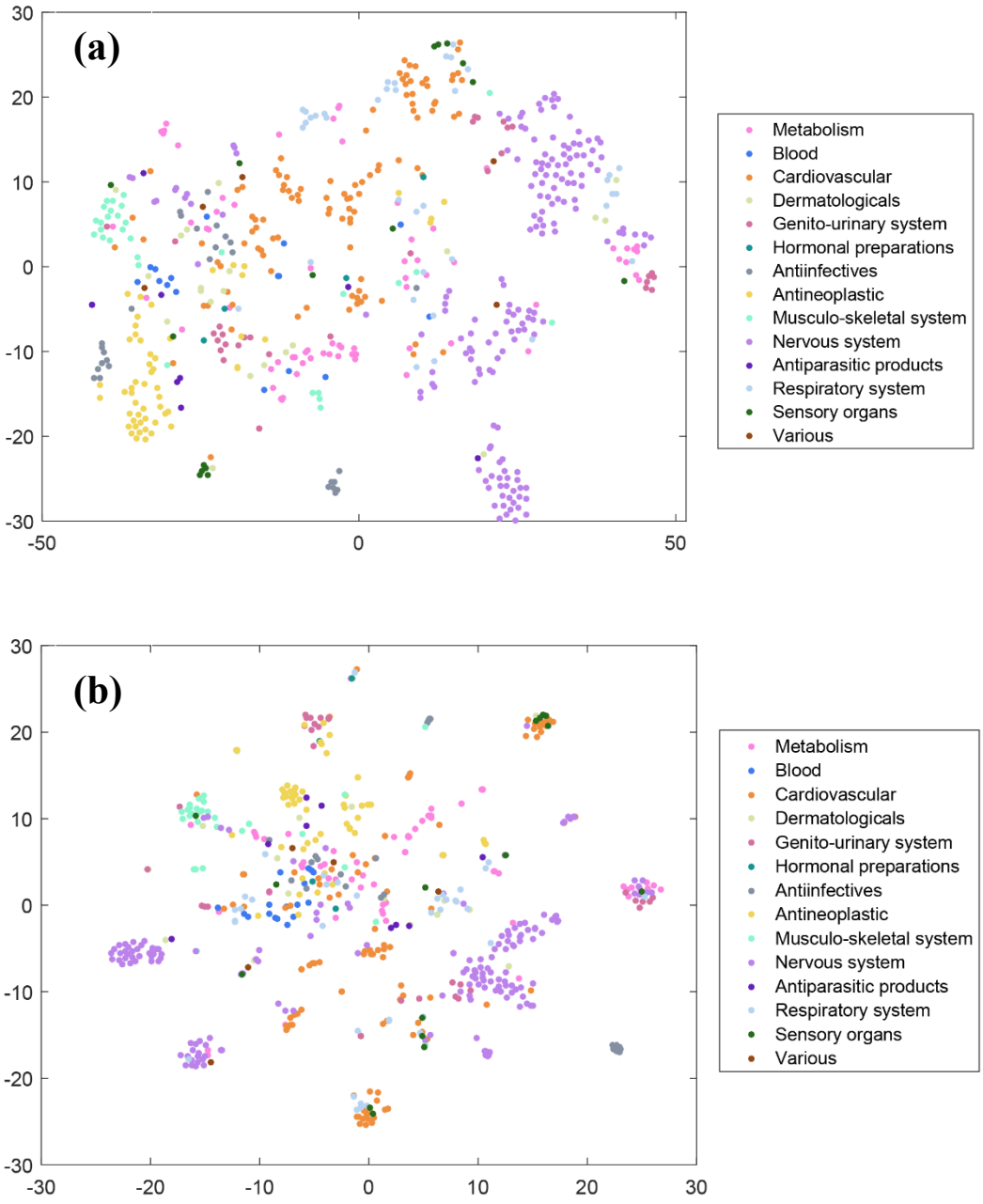


**Figure S1.** (**a**) The two-dimensional (2D) representation of the features learned by multimodal deep autoencoder (MDA) for 14 types of drugs using the t-SNE. (**b**) The two-dimensional (2D) representation of the learned vectors learned by PCA algorithm for 14 types of drugs using the t-SNE. We grouped them by the first-level of the Anatomical Therapeutic Chemical (ATC) Classification System codes.

# Supplementary Tables

**Table S1**. The number of nodes of individual types in the constructed heterogeneous network.

| Type of node | Count |
|---|---|
| Drug | 1,519 |
| Disease | 1,229 |
| Protein | 1,025 |
| Side-effect | 12,904 |
| Total | 16,677 |

**Table S2.** The statistics of individual interactions or association matrices in the constructed heterogeneous network.

| Type of edge | Count |
|---|---|
| Drug-Disease | 6,677 |
| Drug-Drug | 290,836 |
| Drug-Protein | 6,744 |
| Drug-Side-effect | 382,041 |
| Total | 686,298 |

**Table S3.** 14 novel drug-disease interactions among the list of top 20 significant predictions derived by deepDR for Alzheimer's Disease that can be supported by previously published studies.

| Rank | Drug name | Predict score | Evidence |
|---|---|---|---|
| 1 | Isoprenaline | 0.670 | [25] |
| 2 | Aripiprazole | 0.523 | [26-28] |
| 3 | Phenobarbital | 0.489 | [29, 30] |
| 4 | Risperidone | 0.489 | [31-33] |
| 5 | Dopamine | 0.475 | [34, 35] |
| 6 | Phenytoin | 0.461 | [36] |
| 7 | Carbamazepine | 0.459 | [37, 38] |
| 8 | Ceftriaxone | 0.439 | [39, 40] |
| 9 | Nitric Oxide | 0.412 | [41-43] |
| 10 | Primidone | 0.412 | NA |
| 11 | Hyoscyamine | 0.406 | NA |
| 12 | Perphenazine | 0.403 | [44] |
| 13 | Quetiapine | 0.401 | [45] |
| 14 | Bosentan | 0.379 | [46, 47] |
| 15 | Lamotrigine | 0.378 | [48-50] |
| 16 | Benzylpenicillin | 0.377 | NA |
| 17 | Methylphenobarbital | 0.376 | NA |
| 18 | Biperiden | 0.367 | [51, 52] |
| 19 | Cimetidine | 0.364 | NA |
| 20 | ziprasidone | 0.362 | NA |

**Table S4.** 14 novel drug-disease interactions among the list of top 20 significant predictions derived by deepDR for Parkinson's disease that can be supported by previously published studies.

| Rank | Drug name | Predict score | Evidence |
|---|---|---|---|
| 1 | Orphenadrine | 0.922 | [53, 54] |
| 2 | Metixene | 0.856 | [55, 56] |
| 3 | Pergolide | 0.843 | [57-59] |
| 4 | Cysteine hydrochloride | 0.828 | NA |
| 5 | L-Cysteine | 0.773 | [60] |
| 6 | Acetylcysteine | 0.765 | [61-63] |
| 7 | Diazepam | 0.669 | [64] |
| 8 | Phentermine | 0.596 | [65] |
| 9 | Terazosin | 0.590 | NA |
| 10 | Dextroamphetamine | 0.543 | [66] |
| 11 | Methylphenidate | 0.530 | [67-69] |
| 12 | Dobutamine | 0.525 | [70, 71] |
| 13 | Doxazosin | 0.519 | [72] |
| 14 | Amphetamine | 0.514 | [66, 73] |
| 15 | Tadalafil | 0.509 | NA |
| 16 | Dutasteride | 0.497 | [74, 75] |
| 17 | Alfuzosin | 0.470 | NA |
| 18 | Enalaprilat | 0.463 | NA |
| 19 | Silodosin | 0.437 | NA |
| 20 | Tamsulosin | 0.432 | [76] |

**Table S5.** The area under the receiver operating characteristic curve (AUROC) and the area under precision-recall curve (AUPR) during cross-validation on the gold standard drug-disease network. We performed 10 times of random 5-fold cross-validation and standard derivation (SD) was provided.

| Methods | AUROC±SD | AUPR±SD |
|---|---|---|
| **deepDR** | **0.908±0.0032** | **0.923±0.0028** |
| DTINet | 0.862+0.0023 | 0.892+0.0026 |
| KBMF | 0.791±0.0034 | 0.826±0.0029 |
| RF | 0.783±0.0026 | 0.805±0.0027 |
| SVM | 0.771±0.0031 | 0.778±0.0035 |
| RWR | 0.708±0.0041 | 0.734±0.0053 |
| Katz | 0.724±0.0036 | 0.741±0.0049 |

**Table S6.** We designed different architectures of MDA and used the same setting of cVAE to find the best architecture of MDA. We mainly show the parameter selection process in the refinement step of cVAE, since its results are more striking. The architecture and parameters of cVAE in this step was set according to the previous experimental experience. Each row represents different architecture of MDA, each column represents different iteration of cVAE. We can find that as the iteration of cVAE increase, the performance of each architecture all improving. To ensure the convergence of cVAE, we fixed the number of iterations 500, and find MDA3 achieve the best performance, so we choose it as the MDA architecture.

| | AUROC | AUPR | AUROC | AUPR | AUROC | AUPR |
|---|---|---|---|---|---|---|
| | 100 | | 300 | | 500 | |
| MDA1 | 0.8599 | 0.8925 | 0.8607 | 0.9067 | 0.8668 | 0.9042 |
| MDA2 | 0.8587 | 0.8898 | 0.8630 | 0.9087 | 0.8712 | 0.9077 |
| MDA3 | 0.8575 | 0.8898 | 0.8633 | 0.9099 | **0.8741** | **0.9102** |
| MDA4 | 0.8628 | 0.8934 | 0.8631 | 0.9091 | 0.8707 | 0.9073 |
| MDA5 | 0.8545 | 0.8893 | 0.8625 | 0.9085 | 0.8708 | 0.9075 |

Note:

MDA1: 9*1519, 9*100

MDA2: 9*1519, 9*1000, 9*100

MDA3: 9*1519, 9*1000, 9*500, 9*100

MDA4: 9*1519, 9*1000, 9*500, 9*200, 9*100

MDA5: 9*1519, 9*1000, 9*800, 9*500, 9*200, 9*100

**Table S7.** We use the features extracted from MDA and change the iteration of cVAE to find the best iteration of cVAE.

| Iteration | AUROC | AUPR |
|---|---|---|
| 400 | 0.8679 | 0.9006 |
| 500 | **0.8741** | **0.9102** |
| 600 | 0.8741 | 0.9067 |
| 700 | 0.8725 | 0.9016 |

**Table S8.** We fix the iteration to be 500 and change the architecture of cVAE.

| Architecture | AUROC | AUPR |
|---|---|---|
| 1519 1000 100 | **0.8741** | **0.9102** |
| 1519 1000 500 100 | 0.8333 | 0.8802 |
| 1519 1000 200 100 | 0.8532 | 0.8954 |
| 1519 1000 500 200 100 | 0.8283 | 0.8729 |

**Table S9.** We perform a grid search on hyperparameters α and β of cVAE. α is a parameter to balance between positive samples and negative samples, and β is a parameter introduced to control the strength of regularization. Each row represents different value of α, each column represents different value of β.

| | AUROC | AUPR | AUROC | AUPR | AUROC | AUPR | AUROC | AUPR | AUROC | AUPR |
|---|---|---|---|---|---|---|---|---|---|---|
| | 0 | | 0.5 | | 1 | | 2 | | 3 | |
| 1 | 0.8245 | 0.8649 | 0.8694 | 0.9000 | 0.8602 | 0.9015 | 0.8635 | 0.9087 | 0.8518 | 0.9031 |
| 2 | 0.8347 | 0.8727 | 0.8940 | 0.9136 | 0.8826 | 0.9092 | 0.8724 | 0.9098 | 0.8664 | 0.9089 |
| 5 | 0.8457 | 0.8808 | 0.9054 | 0.9212 | 0.9004 | 0.9180 | 0.8969 | 0.9188 | 0.8879 | 0.9156 |
| 8 | 0.8532 | 0.8858 | **0.9079** | **0.9226** | 0.9030 | 0.9199 | 0.9034 | 0.9226 | 0.8993 | 0.9223 |
| 11 | 0.8622 | 0.8911 | 0.9024 | 0.9177 | 0.9058 | 0.9203 | 0.9033 | 0.9200 | 0.9025 | 0.9215 |
| 15 | 0.8633 | 0.8927 | 0.9053 | 0.9200 | 0.9038 | 0.9193 | 0.9055 | 0.9232 | 0.9044 | 0.9216 |

## Supplementary References


1. Law, V., et al., DrugBank 4.0: shedding new light on drug metabolism. Nucleic Acids Res, 2014. **42**(Database issue): p. D1091-7.
2. Zhu, F., et al., Therapeutic target database update 2012: a resource for facilitating target-oriented drug discovery. Nucleic Acids Res, 2012. **40**(Database issue): p. D1128-36.
3. Hernandez-Boussard, T., et al., The pharmacogenetics and pharmacogenomics knowledge base: accentuating the knowledge. Nucleic Acids Res, 2008. **36**(Database issue): p. D913-8.
4. Gaulton, A., et al., ChEMBL: a large-scale bioactivity database for drug discovery. Nucleic Acids Research, 2012. **40**(D1): p. D1100-D1107.
5. Liu, T.Q., et al., BindingDB: a web-accessible database of experimentally determined protein-ligand binding affinities. Nucleic Acids Research, 2007. **35**: p. D198-D201.
6. Pawson, A.J., et al., The IUPHAR/BPS Guide to PHARMACOLOGY: an expert-driven knowledgebase of drug targets and their ligands. Nucleic Acids Research, 2014. **42**(D1): p. D1098-D1106.
7. Apweiler, R., et al., UniProt: the Universal Protein knowledgebase.

Nucleic Acids Research, 2004. **32**: p. D115-D119.

8. Bodenreider, O., The Unified Medical Language System (UMLS): integrating biomedical terminology. Nucleic Acids Res, 2004. **32**(Database issue): p. D267-70.
9. Cheng, F., et al., Prediction of polypharmacological profiles of drugs by the integration of chemical, side effect, and therapeutic space. J Chem Inf Model, 2013. **53**(4): p. 753-62.
10. Davis, A.P., et al., The Comparative Toxicogenomics Database: update 2011. Nucleic Acids Res, 2011. **39**(Database issue): p. D1067-72.
11. Tatonetti, N.P., et al., Data-driven prediction of drug effects and interactions. Sci Transl Med, 2012. **4**(125): p. 125ra31.
12. Kuhn, M., et al., A side effect resource to capture phenotypic effects of drugs. Mol Syst Biol, 2010. **6**: p. 343.
13. O'Boyle, N.M., et al., Open Babel: An open chemical toolbox. J Cheminform, 2011. **3**: p. 33.
14. Willett, P., Similarity-based virtual screening using 2D fingerprints. Drug Discov Today, 2006. **11**(23-24): p. 1046-53.
15. Smith, T.F. and M.S. Waterman, Identification of common molecular subsequences. J Mol Biol, 1981. **147**(1): p. 195-7.
16. Wang, J.Z., et al., A new method to measure the semantic similarity of GO terms. Bioinformatics, 2007. **23**(10): p. 1274-81.
17. Yu, G., et al., GOSemSim: an R package for measuring semantic similarity among GO terms and gene products. Bioinformatics, 2010. **26**(7): p. 976-8.
18. Luo, Y.A., et al., A network integration approach for drug-target interaction prediction and computational drug repositioning from heterogeneous information. Nature Communications, 2017. **8**.
19. Gönen, M., S.A. Khan, and S. Kaski. Kernelized bayesian matrix factorization. in International Conference on Machine Learning. 2013.
20. Köhler, S., et al., Walking the Interactome for Prioritization of Candidate

Disease Genes. The American Journal of Human Genetics, 2008. **82**(4): p. 949-958.

21. Cao, M., et al., New directions for diffusion-based network prediction of protein function: incorporating pathways with confidence. Bioinformatics, 2014. **30**(12): p. i219-27.
22. U Martin, S.B., et al., Prediction and validation of gene-disease associations using methods inspired by social network analyses. 2013. **8**(9): p. e58977.
23. Breiman, L., Random Forests. Machine Learning, 2001. **45**(1): p. 5-32.
24. Cortes, C. and V. Vapnik, Support-vector networks. Machine Learning, 1995. **20**(3): p. 273-297.
25. Ohm, T.G., J. Bohl, and B. Lemmer, Reduced basal and stimulated (isoprenaline, Gpp(NH)p, forskolin) adenylate cyclase activity in Alzheimer's disease correlated with histopathological changes. Brain Res, 1991. **540**(1-2): p. 229-36.
26. De Deyn, P., et al., Aripiprazole for the Treatment of Psychosis in Patients With Alzheimer's Disease: A Randomized, Placebo-Controlled Study. Journal of Clinical Psychopharmacology, 2005. **25**(5).
27. De Deyn, P.P., et al., Aripiprazole in the treatment of Alzheimer's disease. Expert Opinion on Pharmacotherapy, 2013. **14**(4): p. 459-474.
28. Streim, J.E., et al., A Randomized, Double-Blind, Placebo-Controlled Study of Aripiprazole for the Treatment of Psychosis in Nursing Home Patients with Alzheimer Disease. The American Journal of Geriatric Psychiatry, 2008. **16**(7): p. 537-550.
29. Cumbo, E. and L.D. Ligori, Levetiracetam, lamotrigine, and phenobarbital in patients with epileptic seizures and Alzheimer's disease. Epilepsy & Behavior, 2010. **17**(4): p. 461-466.
30. Brodie, M.J. and P. Kwan, Current position of phenobarbital in epilepsy and its future. Epilepsia, 2012. **53 Suppl 8**: p. 40-6.
31. Negron, A.E. and W.E. Reichman, Risperidone in the treatment of

patients with Alzheimer's disease with negative symptoms. Int Psychogeriatr, 2000. **12**(4): p. 527-36.

32. Katz, I., et al., The efficacy and safety of risperidone in the treatment of psychosis of Alzheimer's disease and mixed dementia: a meta-analysis of 4 placebo-controlled clinical trials. International Journal of Geriatric Psychiatry, 2007. **22**(5): p. 475-484.
33. Meguro, K., et al., Risperidone is Effective for Wandering and Disturbed Sleep/Wake Patterns in Alzheimer's Disease. Journal of Geriatric Psychiatry and Neurology, 2004. **17**(2): p. 61-67.
34. Li, J.I.E., et al., Dopamine and L-dopa disaggregate amyloid fibrils: implications for Parkinson's and Alzheimer's disease. The FASEB Journal, 2004. **18**(9): p. 962-964.
35. Walker, Z., et al., Differentiation of dementia with Lewy bodies from Alzheimer's disease using a dopaminergic presynaptic ligand. J Neurol Neurosurg Psychiatry, 2002. **73**(2): p. 134-40.
36. Dhikav, V., Can phenytoin prevent Alzheimer's disease? Med Hypotheses, 2006. **67**(4): p. 725-8.
37. Olin, J.T., et al., A Pilot Randomized Trial of Carbamazepine for Behavioral Symptoms in Treatment-Resistant Outpatients with Alzheimer Disease. The American Journal of Geriatric Psychiatry, 2001. **9**(4): p. 400-405.
38. Gleason, R.P. and L.S. Schneider, Carbamazepine treatment of agitation in Alzheimer's outpatients refractory to neuroleptics. J Clin Psychiatry, 1990. **51**(3): p. 115-8.
39. Zumkehr, J., et al., Ceftriaxone ameliorates tau pathology and cognitive decline via restoration of glial glutamate transporter in a mouse model of Alzheimer's disease. Neurobiol Aging, 2015. **36**(7): p. 2260-2271.
40. Koomhin, P., K. Tilokskulchai, and S.J.S. Tapechum, Ceftriaxone improves spatial learning and memory in chronic cerebral hypoperfused rats. 2012. **38**(4): p. 356.

41. Law, A., S. Gauthier, and R. Quirion, Say NO to Alzheimer's disease: the putative links between nitric oxide and dementia of the Alzheimer's type. Brain Research Reviews, 2001. **35**(1): p. 73-96.
42. de la Torre, J.C. and G.B. Stefano, Evidence that Alzheimer's disease is a microvascular disorder: the role of constitutive nitric oxide. Brain Research Reviews, 2000. **34**(3): p. 119-136.
43. Malinski, T., Nitric oxide and nitroxidative stress in Alzheimer's disease. Journal of Alzheimers Disease, 2007. **11**(2): p. 207-218.
44. Baumann, P., C.B. Eap, and D.F. Zullino, Fluvoxamine and perphenazine for psychosis in Alzheimer's disease: pharmacokinetic considerations. J Nerv Ment Dis, 2001. **189**(11): p. 798-9.
45. Scharre, D.W. and S.I. Chang, Cognitive and behavioral effects of quetiapine in Alzheimer disease patients. Alzheimer Dis Assoc Disord, 2002. **16**(2): p. 128-30.
46. Palmer, J. and S. Love, Endothelin receptor antagonists: potential in Alzheimer's disease. Pharmacol Res, 2011. **63**(6): p. 525-31.
47. Elesber, A.A., et al., Bosentan preserves endothelial function in mice overexpressing APP. Neurobiology of Aging, 2006. **27**(3): p. 446-450.
48. Suzuki, H. and Y. Inoue, A Comparison of Lamotrigine or Sodium Valproate on the Efficacy in Alzheimer's disease with Behavioral and Psychological Symptoms of Dementia: A Retrospective Open-Label Study Running Title: Efficacy of Anticonvulsants for BPSD. Journal of Gerontology & Geriatric Research, 2015. **04**(06).
49. Tekin, S., et al., Antiglutamatergic therapy in Alzheimer's disease--effects of lamotrigine. Short communication. J Neural Transm (Vienna), 1998. **105**(2-3): p. 295-303.
50. De León, O.A., Treatment of Psychotic Symptoms With Lamotrigine in Alzheimer Disease. J Clin Psychopharmacol, 2004. **24**(2).
51. Wezenberg, E., et al., Modulation of memory and visuospatial processes by biperiden and rivastigmine in elderly healthy subjects. 2005. **181**(3):

p. 582-594.

52. Sambeth, A., et al., Biperiden selectively induces memory impairment in healthy volunteers: no interaction with citalopram. Psychopharmacology (Berl), 2015. **232**(11): p. 1887-97.

53. Strang, R.R., ORPHENADRINE IN THE TREATMENT OF PARKINSON'S DISEASE. Curr Med Drugs, 1964. **5**(1): p. 24-31.

54. Bassi, S., et al., Treatment of Parkinson's disease with orphenadrine alone and in combination with L-dopa. Br J Clin Pract, 1986. **40**(7): p. 273-5.

55. National Center for Biotechnology Information. PubChem Database. Metixene, CID=4167. (accessed on Mar. 23, 2019)]. Available from: https://pubchem.ncbi.nlm.nih.gov/compound/4167.

56. https://www.drugbank.ca/drugs/DB00340

57. Van Camp, G., et al., Treatment of Parkinson's disease with pergolide and relation to restrictive valvular heart disease. The Lancet, 2004. **363**(9416): p. 1179-1183.

58. Storch, A., et al., High-dose treatment with pergolide in Parkinson's disease patients with motor fluctuations and dyskinesias. Parkinsonism Relat Disord, 2005. **11**(6): p. 393-8.

59. Goetz, C.G., et al., Pergolide in Parkinson's Disease. Archives of Neurology, 1983. **40**(13): p. 785-787.

60. Zhang, F. and G. Dryhurst, Effects of L-Cysteine on the Oxidation Chemistry of Dopamine: New Reaction Pathways of Potential Relevance to Idiopathic Parkinson's Disease. Journal of Medicinal Chemistry, 1994. **37**(8): p. 1084-1098.

61. Coles, L.D., et al., Repeated-Dose Oral N-Acetylcysteine in Parkinson's Disease: Pharmacokinetics and Effect on Brain Glutathione and Oxidative Stress. J Clin Pharmacol, 2018. **58**(2): p. 158-167.

62. Katz, M., et al., Cerebrospinal fluid concentrations of N-acetylcysteine after oral administration in Parkinson's disease. Parkinsonism Relat

Disord, 2015. **21**(5): p. 500-3.

63. Monti, D.A., et al., N-Acetyl Cysteine May Support Dopamine Neurons in Parkinson's Disease: Preliminary Clinical and Cell Line Data. PLoS One, 2016. **11**(6): p. e0157602.
64. Pourcher, E., et al., Effects of ethybenztropine and diazepam on levodopa-induced diphasic dyskinesia in Parkinson's disease. Vol. 4. 1989. 195-201.
65. Barmore, R., et al., A Case of Tardive Dyskinesia and Parkinsonism Following Use of Phentermine for Weight Loss (P4.082). Neurology, 2018. **90**(15 Supplement): p. P4.082.
66. Parkes, J.D., et al., Amphetamines in the treatment of Parkinson's disease. Journal of neurology, neurosurgery, and psychiatry, 1975. **38**(3): p. 232-237.
67. Mendonça, D.A., K. Menezes, and M.S. Jog, Methylphenidate improves fatigue scores in Parkinson disease: A randomized controlled trial. Movement Disorders, 2007. **22**(14): p. 2070-2076.
68. Devos, D., et al., Methylphenidate : a treatment for Parkinson's disease? CNS Drugs, 2013. **27**(1): p. 1-14.
69. Auriel, E., J.M. Hausdorff, and N. Giladi, Methylphenidate for the treatment of Parkinson disease and other neurological disorders. Clin Neuropharmacol, 2009. **32**(2): p. 75-81.
70. Nakamura, T., et al., Dobutamine stress test unmasks cardiac sympathetic denervation in Parkinson's disease. J Neurol Sci, 2007. **263**(1-2): p. 133-8.
71. Nakamura, T., et al., Cardiac sympathetic denervation detected with dobutamine infusion in patients with Parkinson's disease: Correlation with cardiac <sup>123</sup>I-metaiodobenzylguanidine (MIBG) uptake; A follow-up report. Autonomic Neuroscience: Basic and Clinical, 2007. **137**(1): p. 105.
72. Gomes, C.M., et al., Neurological status predicts response to alpha-

blockers in men with voiding dysfunction and Parkinson's disease. Clinics (Sao Paulo, Brazil), 2014. **69**(12): p. 817-822.

73. Garwood, E.R., et al., Amphetamine exposure is elevated in Parkinson's disease. NeuroToxicology, 2006. **27**(6): p. 1003-1006.
74. Litim, N., et al., The 5alpha-reductase inhibitor Dutasteride but not Finasteride protects dopamine neurons in the MPTP mouse model of Parkinson's disease. Neuropharmacology, 2015. **97**: p. 86-94.
75. Litim, N., et al., Effect of the 5alpha-reductase enzyme inhibitor dutasteride in the brain of intact and parkinsonian mice. J Steroid Biochem Mol Biol, 2017. **174**: p. 242-256.
76. Gorur, S., et al., Effect of tamsulosin therapy on lower urinary tract symptoms in Parkinson's disease. Vol. 34. 2008. 113-117.